Monitoring Tropical Alpine Lake Levels in a Culturally Sensitive Environment Utilizing 3D Technological Approaches

Authors: Delparte, D. M., Belt, M., Nishioka, C., Turner, N., Richardson, R. T., et al.

Monitoring tropical alpine lake levels in a culturally sensitive environment utilizing 3D technological approaches

D. M. Delparte*#

M. Belt*

C. Nishioka†

N. Turner†

R. T. Richardson‡ and

T. Ericksen§

*Geosciences, Idaho State University, 921 South 8th Avenue, STOP 8072, Pocatello, Idaho 83209-8072, U.S.A.
†Spatial Data Analysis and Visualization Lab, University of Hawai`i at Hilo, 200 West Kawili Street, Hilo, Hawai`i 96720, U.S.A.
‡College of Education, Idaho State University, 921 South 8th Avenue, STOP 8059, Pocatello, Idaho 83209-8072, U.S.A.
§Pacific GPS Facility, University of Hawai`i at Mānoa, 1680 East West Road, Honolulu, Hawai`i 96822, U.S.A.
#Corresponding author: delparte@isu.edu

Abstract

Lake Waiau is a tropical alpine lake situated near the summit of Mauna Kea on the Island of Hawai'i at an elevation of 3969 m. The lake is a place of Hawaiian cultural practice that encompasses Hawaiian mythology, history, genealogy, and spirituality. Concern over declining lake levels has created the stimulus to examine methodologies to monitor lake levels without disturbance. The objective of this research study was to determine the most accurate and cost-effective combination of new approaches to enable long-term monitoring with minimal disturbance to the lake and its environs. Three strategies were used to construct 3D models of the lake: soft-copy stereo photogrammetry from aerial photography, image-based 3D reconstruction from overlapping photographs (Structure from Motion), and terrestrial laser scanning (TLS). To supplement these detection methods, side scan sonar was used to collect bathymetric data. The results were three high-resolution 3D models that were used to calculate volumetric and areal changes over time using Geographic Information Systems (GIS) to analyze and visualize the lake body. The methodologies used in this study are compared for the feasibility of long-term data collection based on variations in accuracy and the associated costs of data collection.

Introduction

Lake Waiau is a shallow, tropical alpine lake situated at 3969 m, nestled in the crater of the Pu'u Waiau cinder cone, one of several that form the summit of Mauna Kea, the highest mountain in the Hawaiian Archipelago at 4205 m (Fig. 1). Lake Waiau, as Mauna Kea's sole alpine lake and one of the highest alpine lakes in the United States (Laws and Woodcock, 1981), is a unique locale for study of high-elevation tropical lake dynamics. Maximum lake surface area is approximately 7000 m². The lake is within the Mauna Kea Ice Age Natural Area Reserve, established in 1981, and is managed by the State of Hawai'i, Department of Land and Natural Resources. Lake Waiau has a long history of cultural significance among Native Hawaiians based on nearby archaeological sites, past events, stories, and continued use as a site of spiritual practice (Group 70 International, 2000; Maly and Maly, 2005; Ho'akea, 2009).

Prior Research on Lake Waiau

Studies conducted at this site have been limited, with most of the research conducted prior to 1980. Prior research on the lake and its immediate vicinity can be classified into four generalized categories: (1) cataloging of indigenous organisms, (2) comparative geomagnetic studies, (3) formation and weathering of the summit cone, and (4) examinations of water flow patterns and lake levels. The latter two areas of research are most relevant to this study because their mapping records provide a historical baseline for comparison with the methods used in this study.

The earliest recorded survey of the flora and fauna of Lake Waiau and its environs was conducted by a Hawaiian Academy of Science expedition to Mauna Kea in 1935. The lake supports a unique assemblage of insects and microorganisms. Insects include four species of Cladocera, commonly known as water fleas (Ueno, 1936) and two predacious insects, *Geocoris pallens* and the Wēkiu bug *(Nysius wekiuicola), which is a rare species endemic to the upper slopes of Mauna Kea. Its habitat corresponds with previously glaciated* regions of the upper mountain. Microorganisms include 13 diatom species (Massey, 1978), phytoplankton (*Anabaena, Oscillatoria, Closterium, Cosmarium,* and *Sphaerozonia*) and benthic algal mats consisting of *Gloethece, Phormidium,* and *Anabaena* (Kinzie et al., 1998). A new diatom species, *Stauroneis maunakeäensis*, was discovered by Massey (1978) from Lake Waiau sediment cores. *Laws and Woodcock (1981) documented changes in phytoplankton distribution associated with a period of drought (July 1976–November 1978), where the lake level dropped more than 2 m below its characteristic overflow level, resulting in eutrophication associated with a bloom of Nannochoris bacillaris chlorophytes.*

Lake Waiau sediment cores have provided a 13,000 year paleomagnetic record of geomagnetic variations in the Central Pacific (Peng and King, 1992). They have been used in comparative eomagnetic dipole surveys designed to fabricate predictive models that test records of secular variations of the Earth's geomagnetic
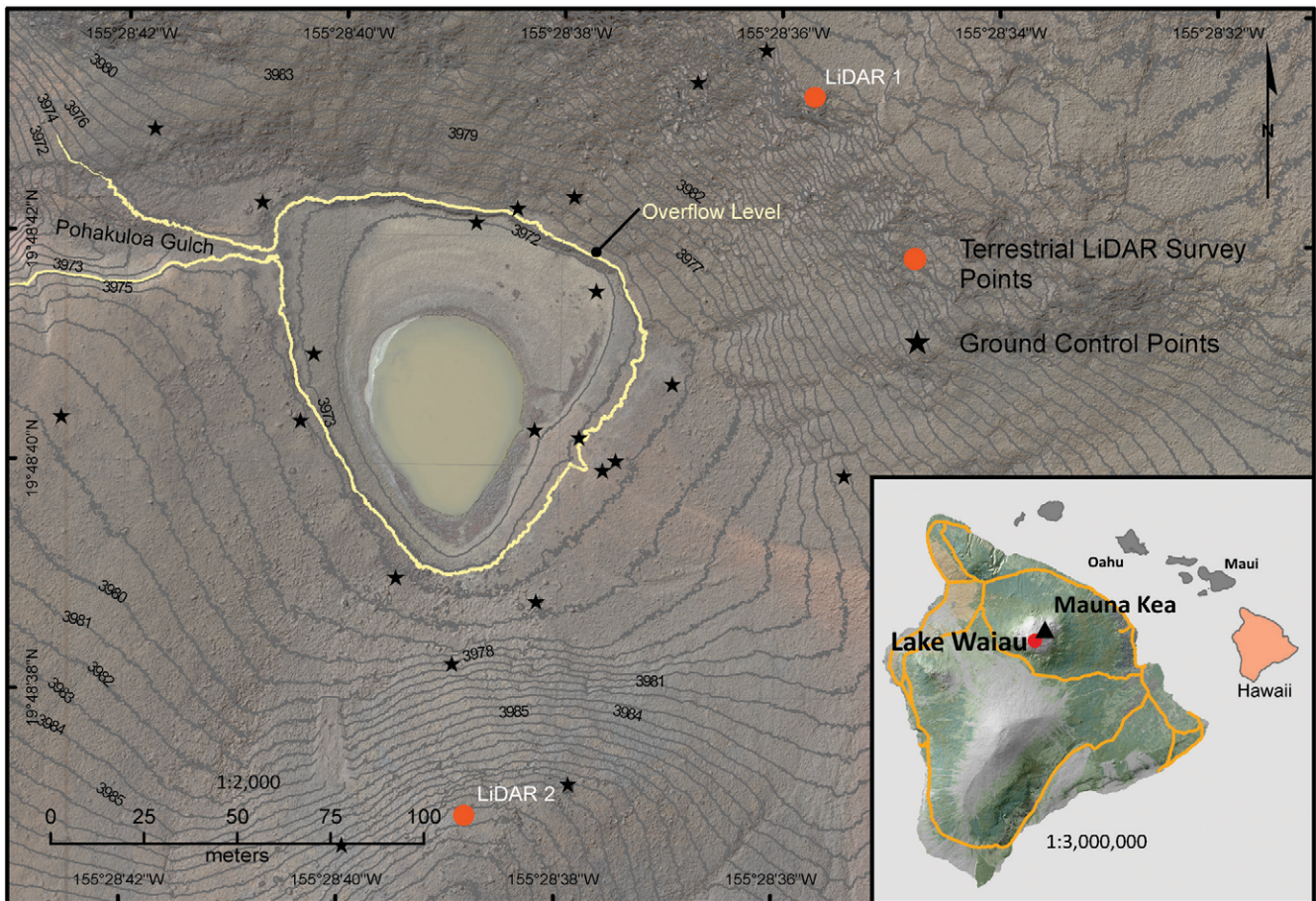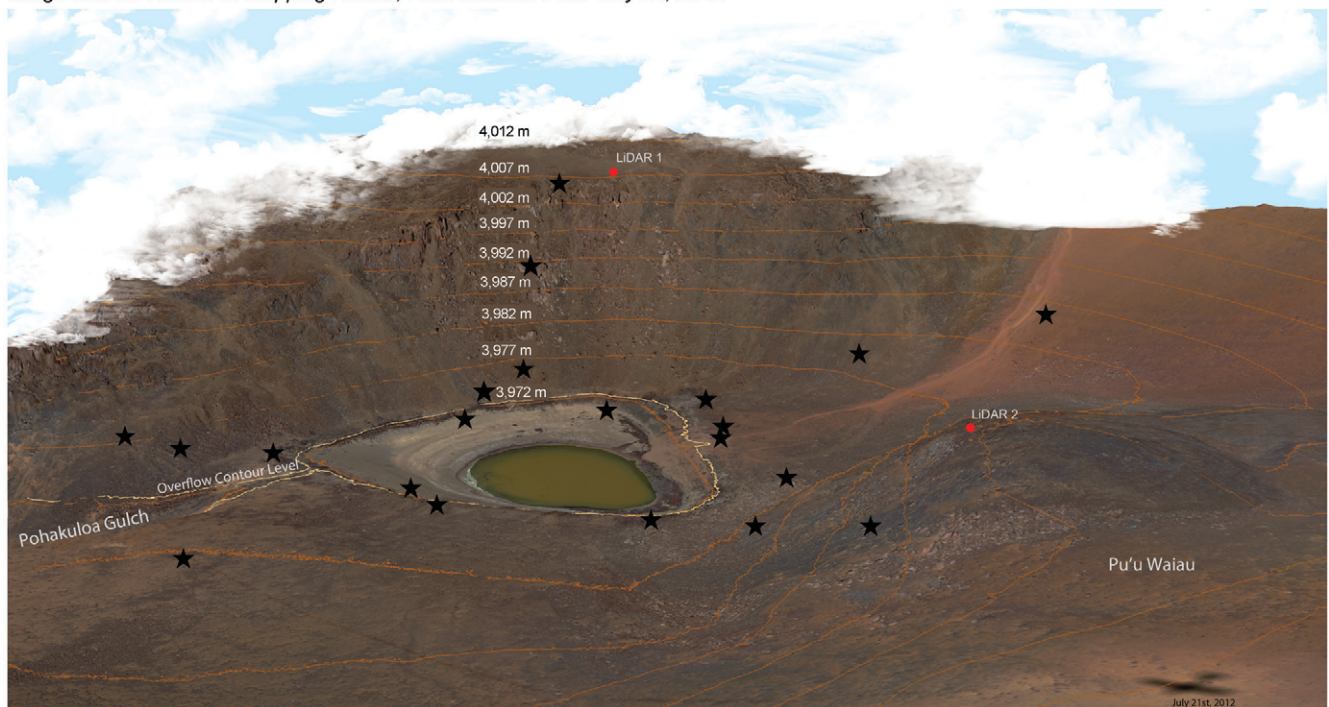
FIGURE 1. Lake Waiau Study Area. 3 cm digital elevation model (DEM) with orthomosaic overlay.

field (Peng and King, 1992; Hagstrum and Champion, 1995; Valet et al., 2008). Sediment core samples have ranged between 1 and 7.5 m in size (Woodcock et al., 1966). Sediments from the lake consist of plagioclase from local tephra, montmorillonite and goethite from weathering of surrounding materials, as well as quartz from eolian action (Fan, 1978). Radiocarbon dating of these sedi-

ments suggests that Lake Waiau is at least 9000 years old, likely originating from the most recent period of glaciation of the summit area (Porter, 1979).

There has been research pertaining to the formation and weathering of the summit area of Mauna Kea and the subsequent orogenic development of Lake Waiau, based on past glaciations. Porter et al. (1977) radioisotope dated four glacial periods: 250,000, 135,000, 55,000, and 20,000 years B.P. Porter (2005) described a characteristic pattern of lava flows covering the most recent glacial Pleistocene and Holocene surfaces. Current surface sediments are volcanic material deposited from volcanic eruptions approximately 4500 years ago, overlaying paleosols formed during the most recent Holocene glaciation of 20,000 years B.P. (Porter, 1971; Wolfe et al., 1997). Woodcock (1974) documented a 10-m-thick permafrost layer at the 4140 m elevation level that is believed to be slowly melting. Located at 0.4 m below the surface, these remnant glacial remains persist in spite of a local annual air temperature of 3.6 °C, which is uncharacteristic of periglacial environments. Woodcock surmised that meltwater from snowfall absorbs and disperses heat that would otherwise melt the permafrost. It has been suggested that an impermeable permafrost layer (Woodcock, 1974, 1980) or ground ice layer (Gregory and Wentworth, 1937) may exist below the lake bottom and act as a seepage barrier. Other researchers proposed that a basalt flow extending down into the Puʻu Waiau cone plus an underlying impermeable substrate (Ugolini, 1974; Porter, 1979; Wolfe et al., 1997) combine to confine water flow within the cone and restrict groundwater loss. This impermeable substrate, a hyaloclastite layer, of fine clay sediments could have formed hydrothermally as steam escaping from the Puʻu Waiau cinder cone. Cinders and ash can be converted to fine clay through magma contact with ground or surface water beneath glacial ice. This layer of relatively impermeable sediments contributes to lake retention, preventing water from percolating downward.

Tracking water level change has yielded a greater understanding of the variations in lake morphology and explanations as to significant fluctuations in water levels. Maciolek (1982) estimated the maximum areal extent of the lake as 7300 m², when overflowing, while Ehlmann et al. (2005) estimated an average lake extent of 6000 m². Woodcock and Groves (1969) recorded a high of 3 m depth during periods of maximum precipitation (December–January), to 2.5 m in the summer due to gradual bottom seepage and evaporation. Other researchers noted much lower lake levels: Woodcock (1980) and Elhmann et al. (2005) reported a significant decrease in lake volume during a period of drought in Hawaii from July 1976 to November 1978, while Ehlmann (2005) observed lake depths of 0.5, 0.8, and 1.04 m for August dates in 1999 to 2001, respectively, with a maximum of 2.35 m in February of 2002. The only documented output source, Pōhakuloa Gulch and its associated springs, flow when the lake crests at over 2.3 m in depth (Woodcock, 1980; Elhmann et al., 2005). Although seepage occurs at lake levels above 1.3 m, evaporation during dry and windy summertime conditions was the leading explanation for the reduction of lake level to less than a third of its winter maximum (Ehlmann et al., 2005). Evidence for evaporation as the primary source of water loss was substantiated by elevated tritium isotope levels (Ehlmann et al., 2005) and hypereutrophication during the drought period recorded by Woodcock (1980). Hypereutrophication accounted for high concentrations of phytoplankton, nitrogen, and sodium (Laws and Woodcock, 1981). Ehlmann's net water balance model offered a good fit with empirical data and led to the conclusion that precipitation captured in the Puʻu Waiau cinder cone was "sufficient to fill and sustain the lake" (Elhmann et al., 2005). Their stream-

flow model was based on field survey data, supplemented by a U.S. Geological Survey 10 m digital elevation model (DEM); this study will present a comparable DEM. Recent Lake Waiau water level declines have generated interest in monitoring and recording further fluctuations in lake level. These declining levels have generally corresponded to varying drought conditions that have persisted since June 2008.

LAKE WAIAU STUDY SITE

Lake Waiau at 3969 m and slightly downslope of the summit of Mauna Kea is located in a tropical alpine desert zone (Fig. 1). Precipitation rates are low, with dry summer months and most precipitation falling as rain or snow in the winter. Lake Waiau has a mean 30 year, annual precipitation of 224.7 mm (Giambelluca et al., 2012). Located above persistent temperature inversions with clear skies and low relative humidity, evaporation rates at summit elevations in Hawaiʻi are high. For example, on the neighboring summit of Mauna Loa at 3400 m, evaporation rates of 6.1 mm per day have been recorded (Bean et al., 1994). Since 2009, Hawaiʻi has experienced several periods of below normal rainfall. The United States Department of Agriculture (USDA) has declared Hawaii County as a disaster area due to drought from a period of January 9, 2012 to January 11, 2013. These dry conditions have dramatically impacted lake levels at Waiau, as the lake depends on precipitation to recharge resulting in the lowest levels observed in recent memory. To monitor the lake level fluctuations, without disturbing this culturally important site, the following technologies were implemented to generate DEMs of the lake and surrounding area. The options selected for this investigation to monitor lake level changes included: terrestrial LiDAR scanning (TLS), Structure from Motion (SfM), and photogrammetry.

Methods

TERRESTRIAL LIDAR SYSTEM (TLS)

Terrestrial Light Detection and Ranging Systems (LiDAR or TLS) have many applications ranging from mining, geology, archaeology, and vegetation surveys to urban planning, forensics, industrial, and structural surveys. The LiDAR unit is ground based and is mounted on a tripod to capture x, y, z (height or elevation) and intensity (i) data from the environment it scans, and it provides a measurement of an object's reflectivity (Campbell, 2007). The Pacific GPS Facility, based at the University of Hawaiʻi at Manoa has an ILRIS-3D portable terrestrial-based LiDAR device manufactured by Optech that was used for this study. The device has a raw range accuracy of 7 mm at 100 m. Laser wavelength is 1535 nm with a range of 1200 m and a maximum density spacing (point-to-point) of 2 cm at 1000 m (Optech Inc., 2012). We conducted laser scans on either side of the lake (Fig. 1). Point-to-point scanning for the two scans ranged from 2.5 cm to 22 cm at the farthest range. The survey data collection was completed on 6 June 2012.

Ground control points (GCPs) were obtained using a Trimble GeoXH with a post-processed estimated horizontal accuracy of 10 cm and vertical accuracy of 10 cm. Combinations of these GCPs were used for georeferencing all of the DEM modeling approaches. To process the x, y, z point cloud data from the TLS, Polyworks software was used to geocorrect the data set. This data set was used as the base layer to align the additional point clouds.
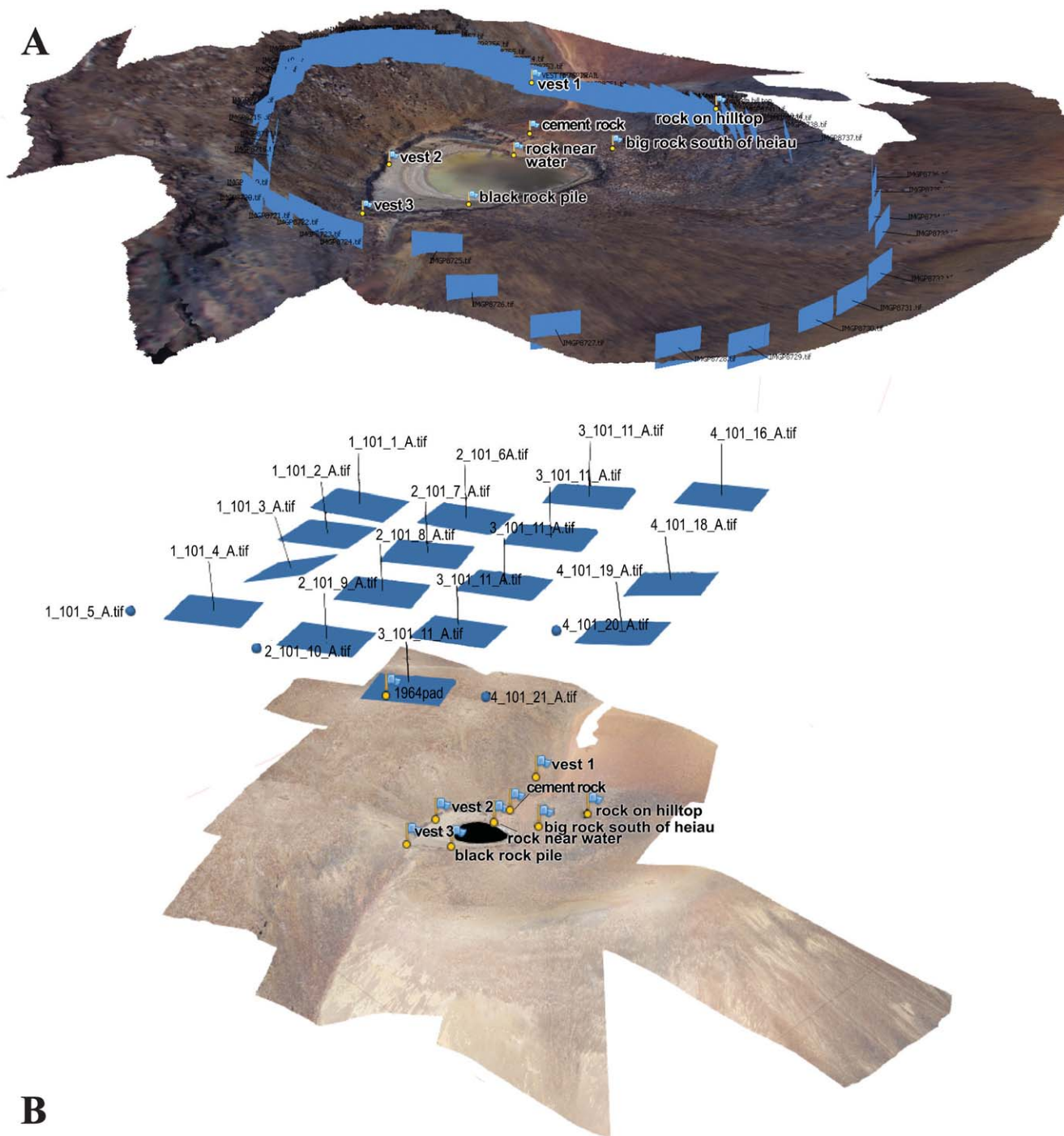
FIGURE 2. Camera positions for structure from motion (SfM) data processing. (A) Camera positions for terrestrial photography SfM DEM generation. (B) Camera positions for aerial photography SfM DEM generation.

STRUCTURE FROM MOTION (SFM)

As a low-cost alternative to terrestrial LiDAR and photogrammetry approaches, recent developments in structure from motion (SfM) technology utilizing photogrammetric reconstruction algorithms and software, such as PhotoScan (www.agisoft.ru), creates digital elevation models from a number of overlapping photographs (Westoby et al., 2012). The elevation or 3D data are obtained through multiple passes over a mapped area, providing both a visual image and a 3D point cloud. To capture the lake using an SfM approach, a series of 57 photos were taken around the lake (Fig. 2) on 21 May 2012 with a Pentax K5 16.1 megapixel (APS-C sensor, crop factor = 1.5×) digital single-lens reflex (DSLR) camera equipped with a 35 mm lens and polarizing filter. All photos were taken at an 18mm focal length @ f5.6 (35mm equivalent = 27mm), which provided a field of view of 29 degrees. Exposure was set at ISO 100 with a white

balance setting for daylight and center weighted average. Fixed aperture priority was chosen to maintain a constant hyper focal distance and to ensure maximum resolution. File output was set to fine JPEG with a dimension of 4928 × 3264 pixels 300 dpi (horizontal/vertical) using 24 bit sRGB color depth. No postprocessing was performed. All Exif (Exchangable image file) metadata tags were captured. A Trimble Explorer Geo XH 6000 series Global Positioning System (GPS) unit was used to record ground control points (GCPs) in the vicinity of the high water mark that could be easily identified throughout each of the photos. Acquisition of NADIR image captures was not feasible, so an average angular perspective of 30 to 45 degrees was used to circumscribe the lake basin at approximately 100 m radial distance from the lake. Figure 2, part A, illustrates the camera positions around the lake.

Using PhotoScan software, a 3D terrain model was created of the study site. Estimate geocorrection error was 0.99 pixel. The resulting georeferenced DEM was exported for comparisons with the other techniques. Structure from motion allows for a fast and inexpensive approach for 3D surface reconstruction with the advantage of requiring only standard photographic images for georeferencing, and Ground Control Points (GCPs).

PHOTOGRAMMETRY

Soft-copy photogrammetry is the process of geometric triangulation of object surface elevations using stereo pairs of imagery (Kasser and Egels, 2002). Soft-copy photogrammetric reconstruction of the Lake Waiau region was accomplished using BAE System SOCET SET 5.6 software with historical aerial imagery captured by NASA Ames Research on 5 September 1995 and scanned into digital images at 1814 dpi resolution. Two photographs of different scale were selected, one captured at 1:14,000 and the other at 1:15,000 from a relative altitude of 7500 ft. The images were captured on 229 mm × 229 mm infrared film using a Wild RC3 metric camera using f = 153.16 mm. SOCET SET image triangulation was successful at achieving an root mean square (RMS) of 0.494 pixels using 507 tie points. Camera position was estimated with the following RMS: Longitude (X) = 0.383 m., Latitude (Y) = 0.310 m, and Elevation (Z) = 0.896 m. DEM processing used the Next Generation Automatic Terrain Extraction (NGATE) algorithm, which calculates pixel-pixel measurements regardless of the output grid spacing. The final DSM yielded a submeter relative error of 0.98 m circular and 0.59 m linear. The final absolute error was 3.04 m circular and 0.84 m linear. An orthomosaic was produced using a most nadir approach with the generated DEM using both original images with a grid spacing of 1 m.

Further aerial photography data was captured by Resource Mapping Hawaii on 21 July 2012. The camera utilized was a PhaseOne 645 DF body and P65+ megapixel near-infrared back. Data were captured in true color and near infrared at an average flying height of 311 m, resulting in a grid spacing of 3 cm. Initial attempts at processing the imagery to create a digital elevation model with softcopy photogrammetry were unsuccessful. Agisoft Photoscan Pro was thus utilized to generate a digital elevation model based on the overlapping 20 image aerial photo data set (Fig. 2, part B). Ground control points were used to georeference the data set with an estimated error of 0.74 pixel. A 3 cm DEM was created.

SONAR

The remotely sensed images and LiDAR were unable to penetrate the depths of Lake Waiau. To acquire bathymetric data, a side scanning sonar device, the Hummingbird 898c SI Combo 7-inch Waterproof Marine GPS and Chartplotter with Sounder, was used to acquire lake depths. A limitation of the device was that areas of the lake with a depth less than ~40 cm could not be recorded. From those lake areas with adequate depth, a 1 m DEM was generated from the sonar data in ArcGIS 10.1. The lake bottom data set was fused with the other DEM data sets to create a seamless surface model of the lake. From this data model, we were able to calculate volumetric measurements based on lake levels.

Results

DEM AND POINT CLOUD COMPARISONS

Four DEM outputs were generated by SfM and terrestrial LiDAR approaches at grid spacing of 3 cm and from the aerial photography at 3 cm and 1 m (Fig. 3). The digital elevation models were generated from the native x, y, and z point clouds and exported into an Esri GRID format. The point cloud resolution around the lake exceeded a point density of 2.5 cm for all models. Due to the nature of the vantage points used during image capture, both resolution and precision of point estimates vary with distance. SfM much like TLS inherently produces clouds of varying point densities characteristic of scene depth. This effect is most noticeable when using sharp oblique angles or near parallel capture positions to the plane of observation as opposed to those of perpendicular orientation to the focal point of the sensor, which will yield higher quality results in scene foregrounds compared to distal regions. Thus, the point densities declined in the models the farther the position away from the focus of the lake center. To create the surface terrain model effect (Fig. 3), hillshades were generated to provide a visual comparison using Esri's ArcGIS software.

To compare metrics between the 3 cm resolution DEMS, ASCII point cloud data was imported into the Open Source CloudCompare (CC) software available through the Open Topography web portal (http://opentopography.org/). We compared the aerial photography SfM model to the terrestrial LiDAR model (TLS) (Fig. 4, part A), the terrestrial SfM to the aerial SfM (Fig. 4, part B), and finally the terrestrial SfM to the TLS model (Fig. 4, part C). The 1 m resolution aerial photography data set was not compared to the higher resolution data sets as the resolutions are too disparate. In order to ensure the best possible comparison, each of the SfM models, after initial georeferencing with the GCPs, were aligned to the TLS data set to minimize introduced positional error from the GPS unit and operator differences in georeferencing. Before alignment, a subsampling of the cropped dense point cloud was performed. This was beneficial in order to speed up computation, which becomes exponentially time consuming if performed with raw points. Since the SfM and LiDAR point clouds are collected in fundamentally different ways, a random subsample of a small percentage of the clouds should suffice as long as relative error between the methods is comparatively small. The cloud to cloud comparison was done to determine the distance between the two clouds of points and how the point clouds may have differed depending on terrain. The results were as follows:

1. Aerial SfM compared to TLS: Mean distance (m) = 0.380, standard deviation = 0.302
2. Terrestrial SfM compared to aerial SfM: Mean distance (m) = 0.173, standard deviation = 0.269
3. Terrestrial SfM compared to TLS: Mean distance (m) = 0.285, standard deviation = 0.262

D. M. DELPARTE ET AL. / 713
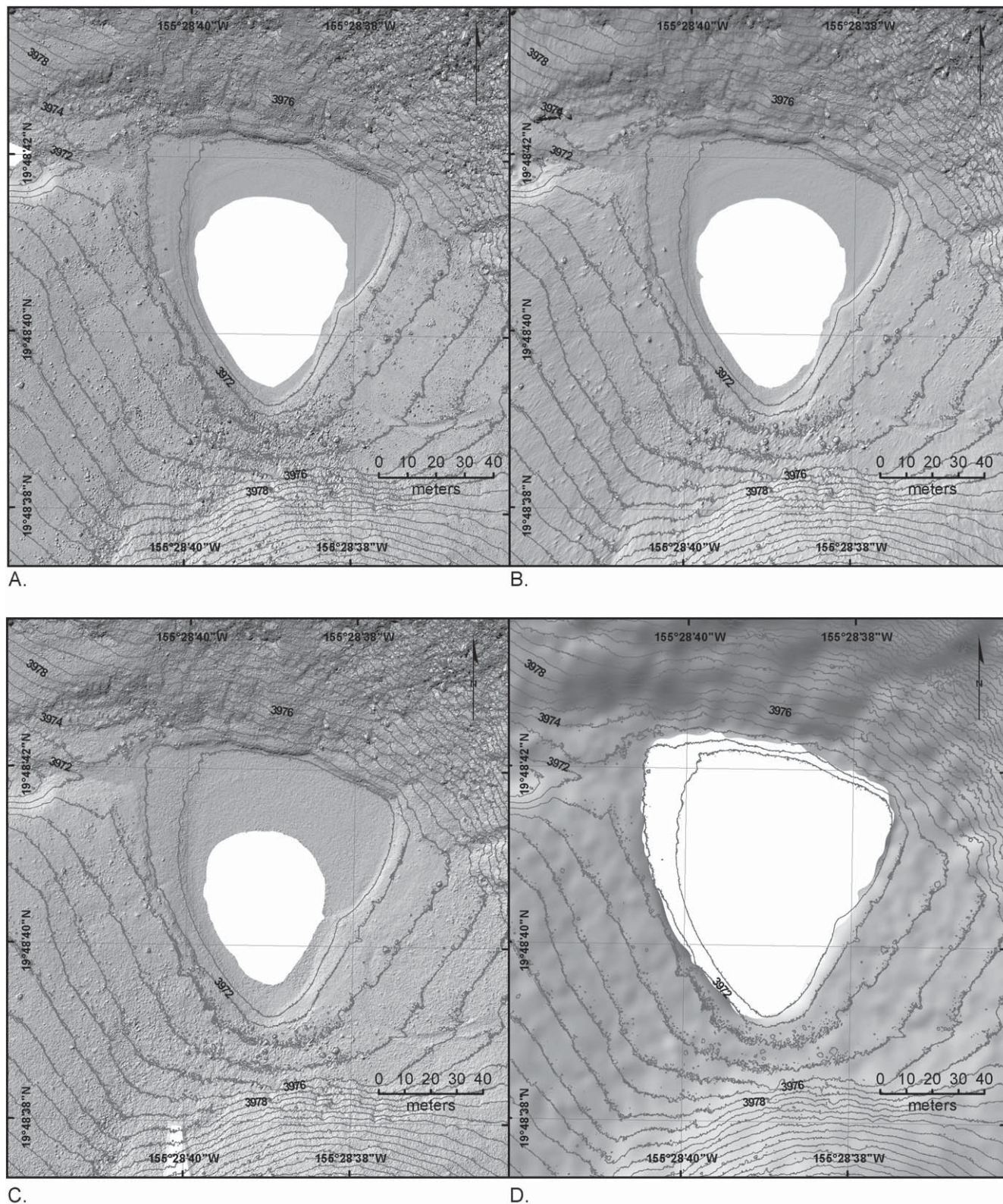
FIGURE 3. Hillshade comparison of DEM data sets. Lake Waiau is the white area in the center of each hillshade and varies in size with date the data was acquired. Contour interval is 1 m. (A) Terrestrial Light Detection and Ranging Systems (LiDAR), 12 June 2012, 3 cm resolution. (B) SfM terrestrial photography, 14 June 2012, 3 cm resolution. (C) SfM terrestrial photography, 19 July 2012, 3 cm resolution. (D) Aerial photography, 9 September 1995, 1 m resolution.
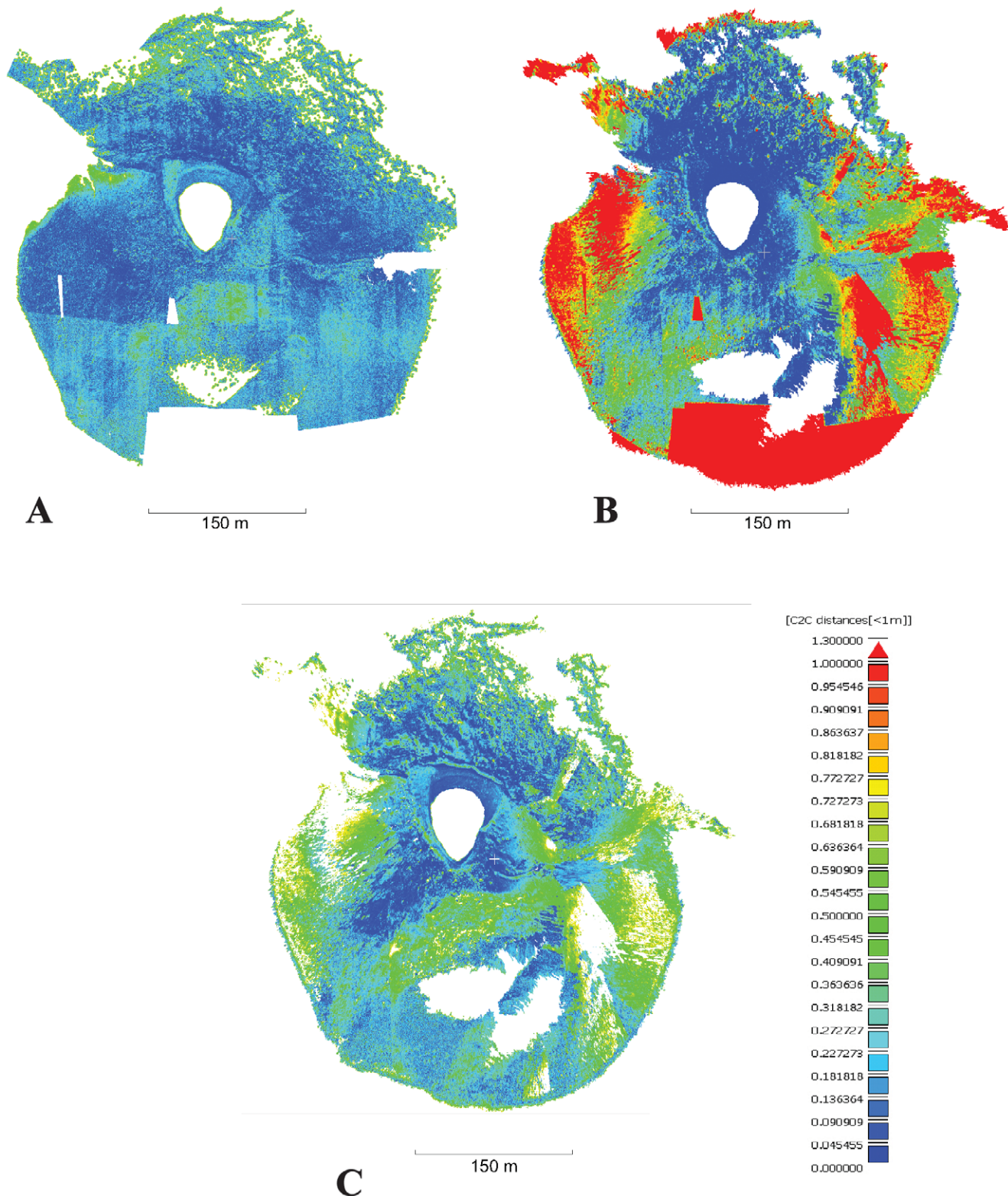
FIGURE 4. Point cloud comparison between the different data collection methods used. (A) Aerial SfM to terrestrial laser scanning (TLS). (B) Terrestrial SfM to aerial SfM. (C) Terrestrial SfM to TLS.

DEM FUSION AND LAKE LEVEL FLUCTUATIONS

Terrestrial LiDAR and SfM methods are unable to capture information below the lake surface. To fill in a seamless representa-

tion of bathymetric data for the lake bottom, sonar data were blended with the TLS and Aerial SfM surface models. In the one month between the TLS and aerial SfM surveys, lake level dropped such that it was possible to incorporate newly exposed lake bed from
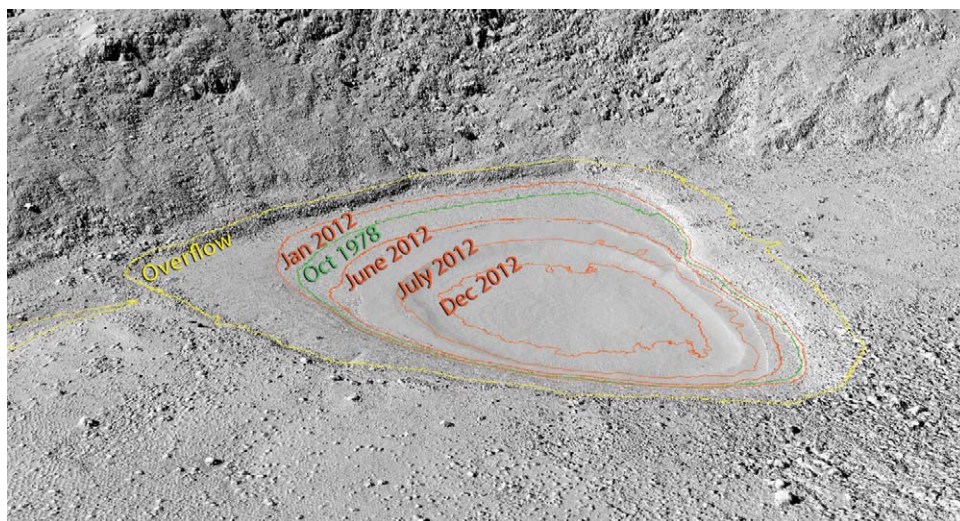
FIGURE 5. DEM fusion of terrestrial LiDAR and sonar lake bathymetry. Lake levels from selected months in 2012 are orange. The overflow level is shown in yellow, and the October 1978 drought level is highlighted in green.

the aerial SfM with TLS and sonar data. Any minor discrepancies between the seams of the data sets were adjusted in ArcGIS using the TLS data set as the base reference. The result of the blending of DEMs is displayed in Figure 5. A smoothing in the lake center is apparent due to the original limitation in the resolution of the sonar data at 1 m.

Contours were generated for lake levels from January to December 2012 as well as identifying the overflow contour and a previous drought level based on a description from Woodcock (1980) (Fig. 5). From these contours and the seamless DEM, volumetrics and maximum depth were identified for each month of 2012. Photographs taken by rangers at the start of each month from the same location guided lake level contour generation (Fig. 6).

Discussion

For this study we were able to successfully integrate several methods of collecting digital elevation and bathymetric data to monitor lake level change without disturbance to the environment or cultural features. Further, we were able to extract volumetric and areal data to measure and monitor declining lake levels. In examining the results, it is evident that the TLS data set provides a more detailed surface model, but the SfM aerial and terrestrial methods are comparable. The point cloud comparisons revealed that the TLS data set had the least difference with the Aerial SfM data. Some of the more steep slopes between these two data sets were likely more detailed from the TLS as opposed to the nadir position of the aerial camera. White areas in the comparison charts indicate zones where data could not be collected. Terrestrial SfM was limited to photography taken from the ground and several areas in white show where regions could not be seen by the camera. As the primary focus for the data collection was around the lake, the least cloud to cloud difference is found here and increases farther away from the lake center. Terrestrial SfM photography also had limitations in areas where the optimal 45 degree angle could not be directed at a target slope. In places where the camera operator was on level ground, the range of the SfM on the opposite slope was reduced and in places created a shadow drift behind rock features revealed in the hillshade representation. Terrestrial and aerial SfM models match closely around the lake (Fig. 3). Areas highlighted in red for the cloud to cloud comparisons between the two SfM methods reveal non-overlapping areas.

Blending digital elevation models collected with varying techniques offers an opportunity to draw from a range of options to collect and monitor landscapes over time. More expensive and time-consuming data collection methods such as terrestrial LiDAR can be supplemented with simple and inexpensive data collection with SfM using a basic camera on the ground. The ability to align data sets to a foundational base data layer offers the opportunity to use a local comparative coordinate reference system from which to measure and detect any changes. As methods of data collection, hardware for processing, software, and techniques to bring together data sets improve, the resulting accuracy should increase. Depending upon the application and accuracy needs for similar studies beyond the scope of this project, our results indicate that a low-cost SfM approach offers a viable option with accuracy close to that of TLS.

The year 2012 has marked a significant decline in Lake Waiau's level in response to lower levels of precipitation. This study has shown that current lake levels are far below the drought level recorded in October 1978 and that the current lake levels are likely some of the lowest in the past several decades. Building a terrain model of Pu'u Waiau facilitates historical comparisons of lake level and assessing changes over time.

Some of the limitations encountered in this study relate to the procedures and technology used. GPS location error will exist from the readings we took of ground control points and subsequently used to georeference the different data sets. By aligning all data to match the TLS data set, this consequence is somewhat mitigated. Improving GPS accuracy with an on-site base station would aid in improving accuracy. Other limitations relate to the nature of the different techniques. Aerial data acquisition facilitates faster data collection over a larger area but has a higher cost. On-the-ground SfM photography is lower cost, but variations in terrain and a reduced ability to cover larger areas creates limitations. However, by blending these data collection techniques, they can become complementary.

Conclusion

Applying new technological approaches to monitoring Lake Waiau offers the opportunity to study the lake without disturbance. Further, the model created provides researchers the
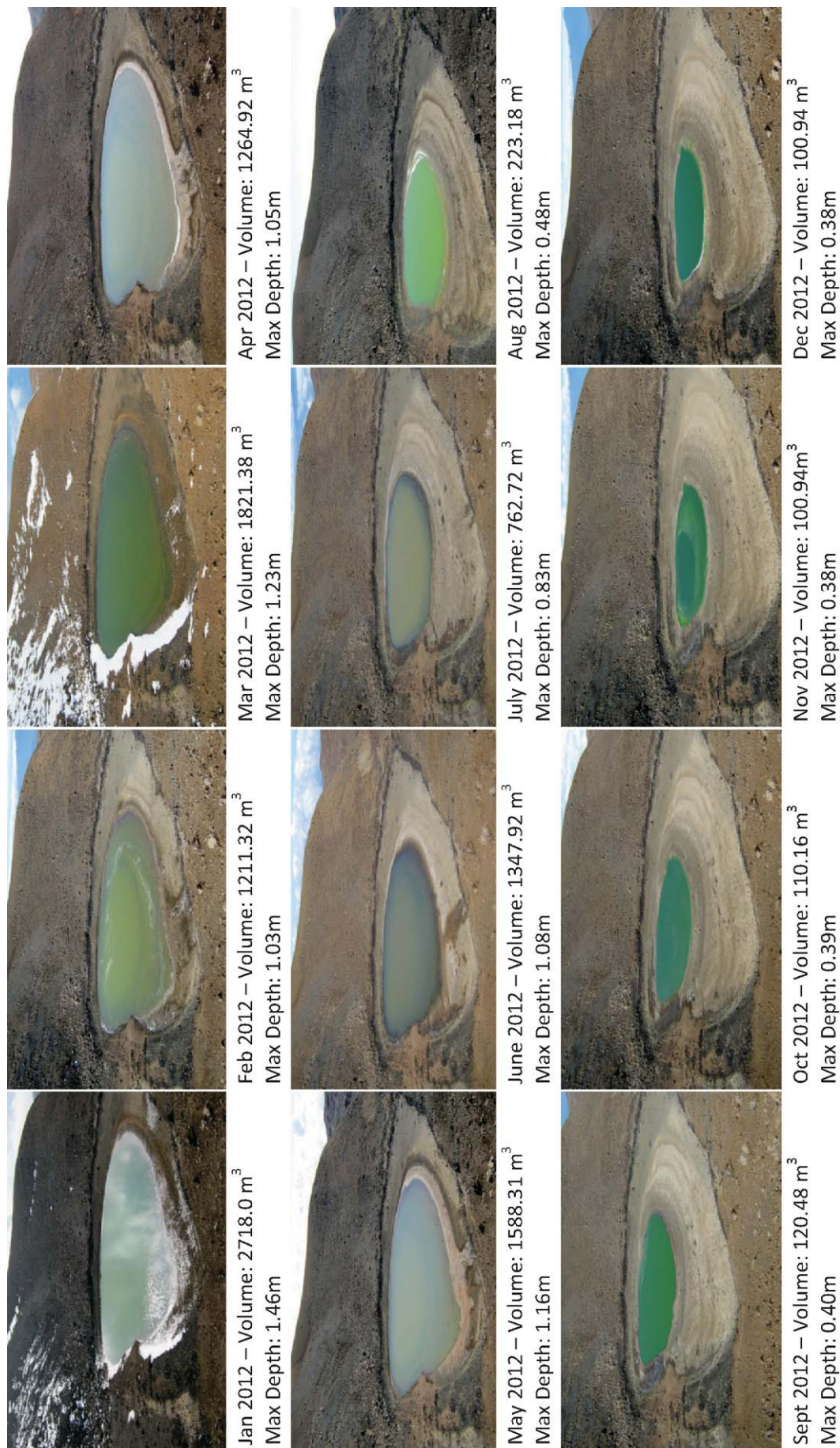
FIGURE 6. Lake Waiau level fluctuations from January 2012 to December 2012. Photography courtesy of the Hawaii Department of Land and Natural Resources, Division of Forestry and Wildlife, Natural Areas Reserve System and the Office of Mauna Kea Management.

Jan 2012 – Volume: 2718.0 m^3
Max Depth: 1.46m

Feb 2012 – Volume: 1211.32 m^3
Max Depth: 1.03m

Mar 2012 – Volume: 1821.38 m^3
Max Depth: 1.23m

Apr 2012 – Volume: 1264.92 m^3
Max Depth: 1.05m

May 2012 – Volume: 1588.31 m^3
Max Depth: 1.16m

June 2012 – Volume: 1347.92 m^3
Max Depth: 1.08m

July 2012 – Volume: 762.72 m^3
Max Depth: 0.83m

Aug 2012 – Volume: 223.18 m^3
Max Depth: 0.48m

Sept 2012 – Volume: 120.48 m^3
Max Depth: 0.40m

Oct 2012 – Volume: 110.16 m^3
Max Depth: 0.39m

Nov 2012 – Volume: 100.94m^3
Max Depth: 0.38m

Dec 2012 – Volume: 100.94 m^3
Max Depth: 0.38m

opportunity to go back in time to compare environmental conditions of today with historical conditions. A recommendation for further study is to begin building a photo database of Lake Waiau to map out and measure how the lake has changed over time, determine the response to climate influences, and forecast challenges in the future.

Acknowledgments

References Cited

Bean, C., Juvik, J. O., and Nullet, D., 1994: Mountain evaporation profiles on the island of Hawai'i. *Journal of Hydrology,* 156(1–4): 181–192.

Campbell, J. B., 2007: *Introduction to Remote Sensing.* New York: Guilford Press.

Elhmann, B. L., Arvidson, R. E., Jolliff, B. L., Johnson, S. S., Ebel, B., Lovenduski, N., Morris, J. D., Byers, J. A., Snider, N. O., and Criss, R. E., 2005: Hydrologic and isotopic modelling of alpine Lake Waiau, Mauna Kea, Hawaii. *Pacific Science,* 59(1): 1–15.

Fan, P.-F., 1978: Mineralogy of sediments from Lake Waiau, Hawaii. *Pacific Science,* 32(2): 219–221.

Giambelluca, T. W., Chen, Q., Frazier, A. G., Price, J. P., Chen, Y.-L., Chu, P.-S., Eischeid, J. K., and Delparte, D. M., 2012: Online rainfall atlas of Hawai'i. *Bulletin of the American Meteorological Society*, 94: 313–316.

Gregory, H. E., and Wentworth, C. K., 1937: General features and glacial geology of Mauna Kea, Hawaii. *Geological Society of America Bulletin,* 48(12): 1719–1742.

Group 70 International, 2000: *Mauna Kea Science Reserve Master Plan.* University of Hawaii, Honolulu.

Hagstrum, J. T., and Champion, D. E., 1995: Late Quaternary geomagnetic secular variation from historical and ^{14}C-dated lava flows on Hawaii. *Journal of Geophysical Research,* 100(B12): 24393–24324, 24403.

Ho'akea, LLC dba Ku'iwalu, 2009: *Mauna Kea Comprehensive Management Plan, UH Management Areas.* University of Hawaii, Office of Mauna Kea Management

Kasser, M., and Egels, Y., 2002: Digital Photogrammetry: London: Taylor & Francis.

Kinzie, R., Banaszak, A., and Lesser, M., 1998: Effects of ultraviolet radiation on primary productivity in a high altitude tropical lake. *Hydrobiologia,* 385(1): 23–32.

Laws, E. A., and Woodcock, A. H., 1981: Hypereutrophication of an Hawaiian alpine lake. *Pacific Science,* 35(3): 257–261.

Maciolek, J. A., 1982: Lakes and lake-like waters of the Hawaiian Archipelago. Bernice P. Bishop Museum, Honolulu, Hawaii.

Maly, K., and Maly, O., 2005: *Mauna Kea-Ka Piko Kaulana O Ka `Āina (Mauna Kea—The Famous Summit of the Land)—A Collection of Native Traditions, Historical Accounts, and Oral History for: Mauna Kea, the Lands of Ka`ohe, Humu`ula and the `Āina Mauna on the Island of Hawaii.* Hilo: The Office of Mauna Kea Management (University of Hawaii-Hilo).

Massey, J. E., 1978: Morphological characteristics of the diatom flora of Lake Waiau: Variation and speciation. *Pacific Science,* 32(2): 215–217.

Optech Inc., 2012: *ILRIS Summary Specification Sheet.* Ontario, Canada.

Peng, L., and King, J. W., 1992: A late Quaternary geomagnetic secular variation record from Lake Waiau, Hawaii, and the question of the Pacific Nondipole Low. *Journal of Geophysical Research–Solid Earth,* 97(B4): 4407–4424.

Porter, S. C., 1971: Holocene eruptions of Mauna Kea Volcano, Hawaii. *Science,* 172(3981): 375–377.

Porter, S. C., 1979: Quaternary stratigraphy and chronology of Mauna Kea, Hawaii: A 380,000-yr record of mid-Pacific volcanism and ice-cap glaciation: Summary. *Geological Society of America Bulletin,* 90(7): 609–611.

Porter, S. C., 2005: Pleistocene snowlines and glaciation of the Hawaiian Islands. *Quaternary International,* 138–139: 118–128.

Porter, S. C., Stuiver, M., and Yang, I. C., 1977: Chronology of Hawaiian glaciations. *Science,* 195(4273): 61–63.

Ueno, M., 1936: *Cladocera of Mauna Kea, Hawaii.* Honolulu: Bernice P. Bishop Museum.

Ugolini, F., 1974: Hydrothermal origin of the clays from the upper slopes of Mauna Kea, Hawaii. *Clay and Clay Minerals,* 22: 189–194.

Valet, J.-P., Herrero-Bervera, E., LeMouël, J.-L., and Plenier, G., 2008: Secular variation of the geomagnetic dipole during the past 2000 years. *Geochemistry, Geophysics, Geosystems,* 9(1): Q01008, doi: http://dx.doi.org/10.1029/2007GC001728.

Westoby, M., Brasington, J., Glasser, N., Hambrey, M., and Reynolds, J., 2012: 'Structure-from-Motion' photogrammetry: a low-cost, effective tool for geoscience applications. *Geomorphology,* 179: 300–314.

Wolfe, E. W., Wise, W. S., and Dalrymple, G. B., 1997: *The Geology and Petrology of Mauna Kea Volcano, Hawaii: A Study of Postshield Volcanism.* U.S. Geological Survey Professional Paper 1557, 129 pp.

Woodcock, A. H., 1974: Permafrost and climatology of a Hawaii volcano crater. *Arctic and Alpine Research,* 6(1): 49–62.

Woodcock, A. H., 1980: Hawaiian alpine lake level, rainfall trends and Spring flow. *Pacific Science,* 34(2): 295–209.

Woodcock, A. and Groves, G. W., 1969: Negative thermal gradient under alpine lake in Hawaii. *Deep-Sea Research*, 16(suppl.): 393-405.

Woodcock, A. H., Rubin, M., and Duce, R. A., 1966: Deep layer of sediments in Alpine Lake in the tropical mid-Pacific. *Science,* 154(3749): 647–648.